

## Simian Virus 40 Transcription in Productively Infected and Transformed Cells

ROBERT A. WEINBERG, ZVI BEN-ISHAI, AND JOHN E. NEWBOLD

*Center for Cancer Research and the Department of Biology, Massachusetts Institute of Technology, Cambridge, Massachusetts 02139; Department of Virology, Hebrew University-Hadassah Medical School, Jerusalem, Israel; and Department of Bacteriology and Immunology, School of Medicine, University of North Carolina, Chapel Hill, North Carolina 27514*

Received for publication 19 December 1973

Several independent cell lines transformed by simian virus 40 carry a species of viral RNA of 900,000 to 1,000,000 daltons. A viral RNA species of similar size is found early in the lytic cycle. Late in the viral lytic cycle, two prominent viral RNA species of about 600,000 and 900,000 daltons are seen. The larger late species shares nucleotide sequences with, and is less stable than, the smaller. These RNA species are located in the cytoplasm of the infected cell. The regions of the viral genome coding for these RNA species are mapped by hybridization of lytic RNA species to fragments of the genome produced by cleavage with *Haemophilus aegyptius* endonuclease.

Simian virus 40 (SV40) demonstrates a productive, lytic infection in monkey kidney cells. Infection of cells from a variety of other mammals leads to transformation of these cells with no production of progeny virus. During the early portion of the lytic cycle, before the onset of viral DNA replication, one species of viral cytoplasmic RNA has been found (42, 43). A species of viral RNA similar in size to early lytic RNA has been observed in mouse 3T3 cells transformed by SV40 (38, 42). The early and transformed viral RNAs sediment as molecules of about 19S, but migrate in acrylamide gels halfway between 18 and 28S rRNA's.

During the late portion of the lytic cycle, two species of viral RNA are observed (38, 42, 43). The smaller of the two late lytic RNAs sediments at 16S in sucrose gradients, but migrates similarly to 18S rRNA in acrylamide gels. The larger of the two late lytic RNAs sediments in sucrose gradients and migrates in gels like the early and transformed viral RNAs. The present studies were designed to investigate the relationship between these four viral RNA species (one transformed, one early lytic, two late lytic).

The interpretation of the present experiments is aided greatly by several recent advances in the field of SV40 transcription: (i) the description of the strand orientation of the SV40 transcription (12, 15, 29); (ii) the use of restriction enzyme fragments to create a map of the SV40 genome (3, 33); and (iii) the use of these fragments in determining the regions of early

and late transcription on the SV40 genome map (13, 30). These studies now indicate that the transcription of the stable, early lytic RNA derives from about 35% of one strand of the SV40 DNA genome. The transcription of stable viral RNA beginning late in the lytic cycle is derived from about 65% of the other strand of the DNA genome. These two regions do not overlap on the genome map. The regions of early and late transcription have now been mapped relative to the restriction enzyme cleavage sites on the viral genome. Additionally, the absolute directions of transcription of the early and late regions relative to the restriction enzyme sites have now been determined (13, 30).

The present report presents information on the size of the viral transcripts made in a variety of virus-transformed cells. Additionally, the size of the early viral RNA is now more precisely demonstrated. Other experiments describe the relative metabolic stability of the two late viral RNAs. A final series of experiments determines the association of the early and late RNAs with different portions of the SV40 genome by hybridizing different lytic RNA species to different genome fragments generated by restriction enzyme cleavage.

### MATERIALS AND METHODS

The majority of the present experiments were performed by using the Sabin small-plaque strain of SV40 derived by M. Vogt. The experiment shown in Fig. 5 was performed by using a small-plaque strain originally obtained from K. Takemoto and further cloned by D. Nathans.

SV40 infections were routinely performed at a multiplicity of 50 to 100 PFU per cell (1). Cell fractionation and extraction of RNA followed the Penman procedure (24, 25). Whole-cell RNA (nucleus + cytoplasm) was extracted by lysis of the monolayer with the sodium dodecyl sulfate (SDS) buffer of Penman (25) containing 1% SDS. This lysate was shaken directly against phenol and chloroform at room temperature. Gel electrophoresis in aqueous medium was performed as previously described (41, 42). Acrylamide gels cast in phosphate-buffered formamide, used only for the experiment of Fig. 5, were prepared as described by Duesberg and Vogt (4) with the following modifications. The formamide gels used here were 2.5% in acrylamide (wt/vol), 0.75% ethylene diacrylate (vol/vol), and the tank buffer contained 0.2% SDS and 1mM EDTA. All gels were fractionated on a Maizel-type Savant gel fractionator. When gel fractions were to be hybridized directly to DNA immobilized on cellulose nitrate filters, the gel fractions were eluted in  $2\times$  SSC (0.3 M NaCl, 0.03 M sodium citrate) with 0.2% SDS. The vials containing the gel fractions were then immersed in boiling water for 15 min to dissolve the gels and reduce the molecular weight of the RNA. DNA-containing filters were then introduced into these vials, and the vials were incubated for 18 h at 65 C. The filters were then exposed to 20  $\mu$ g of pancreatic RNase and 5 U of T1 RNase per ml in  $2\times$  SSC, washed in  $2\times$  SSC + 0.2% SDS, and counted.

Preparation of viral DNA was described in detail by Lindstrom and Dulbecco (15). The preparation of cellulose nitrate filters containing immobilized viral DNA was described by Aloni et al. (1). All SV40 DNA-RNA hybridizations were performed in at least 50-fold DNA excess. Preparation of polyuridylic acid [poly(U)] filters followed Sheldon et al. (35). The use of these filters in the preparation of viral RNA was described by Weinberg et al. (42). Digestion of SV40 DNA with endonuclease Z, and subsequent fractionation of the fragments, was performed by gel electrophoresis as previously described (33). Bands containing DNA fragments in the gels were visualized by ethidium bromide staining and excised (33, 30). The DNA was recovered by further electrophoresis of the excised segments of the gel.

## RESULTS

**Viral RNA in transformed cells.** Virus-transformed cells appear to contain one prominent species of virus-specific RNA. Previous reports (38, 42) indicated that in 3T3 mouse cells transformed by SV40 (SV3T3 cells), a viral RNA species was present which migrates in an acrylamide gel with an electrophoretic mobility halfway between 18 and 28S rRNA's. This result has now been extended to other SV40-transformed cell lines by using the poly(U) filter fractionation technique for the preparation of polyadenylic acid [poly(A)]-associated RNA (35). Labeled RNA from virus-transformed cells is first passed through a

poly(U)-containing filter, and the poly(A)-containing RNA retained on the filter is eluted and run on an acrylamide gel. Each gel fraction is then incubated under hybridizing conditions with a cellulose nitrate filter containing immobilized SV40 DNA. There was SV40 RNA present in a series of independently derived, virus-transformed cell lines (Fig. 1A, B, C), whereas there was an absence of hybridizable RNA in a nontransformed 3T3 mouse cell line (Fig. 1D). In each of the four panels, the profile of the bulk messenger RNA of the cell is shown, and in panels B, C, and D, the profile of late viral RNA from lytically infected cells is also included as a reference marker. Figure 1A shows SV40 homologous RNA from a 3T3 line doubly transformed with both SV40 and polyoma virus. Figure 1B shows the viral RNA from a green monkey line transformed by SV40 (15), and Fig. 1C contains the profile of viral RNA from an SV40-transformed Chinese hamster embryo line. In these and the previously reported SV3T3 experiments (38, 42), one consistently observes a peak of viral RNA migrating halfway between 18 and 28S rRNA's in the acrylamide gel. This peak comigrates with the larger of the two late lytic RNA species. Although we do not preclude the existence of other viral RNA species in virus-transformed cells, we conclude that common to these SV40-transformed cells is a viral RNA species whose molecular weight is estimated at 900,000 to 1,000,000. This RNA species is sufficiently large to contain all of the viral RNA sequences present in those SV40-transformed lines in which 30 to 40% of the viral genome is transcribed (1, 12, 18, 19, 23, 24, 31). As such, it may be the sole viral mRNA species present in those lines.

**Early lytic RNA.** Previous experiments suggested that early lytic RNA is of a similar size to viral RNA from transformed cells (38, 43). This is demonstrated more directly here. The RNA analyzed in Fig. 2 was prepared by poly(U) fractionation. The heterogeneous profiles shown in Fig. 2 are those of the bulk messenger RNA from infected cells. Figures 2a and b show hybridizable RNA from BSC-1 monkey kidney cells infected with SV40 virus and labeled from 1 to 8 (Fig. 2a) and from 8 to 14 h postinfection (Fig. 2b). Figure 2c shows viral RNA in BSC-1 cells which were infected in the presence of cytosine arabinoside, an inhibitor of DNA synthesis known to inhibit late viral function and transcription (2, 14, 32). The cells were labeled from 14 to 20 h postinfection in the continued presence of the drug.

Very early in the lytic cycle we were not able to detect a peak of viral RNA (Fig. 2a; see also

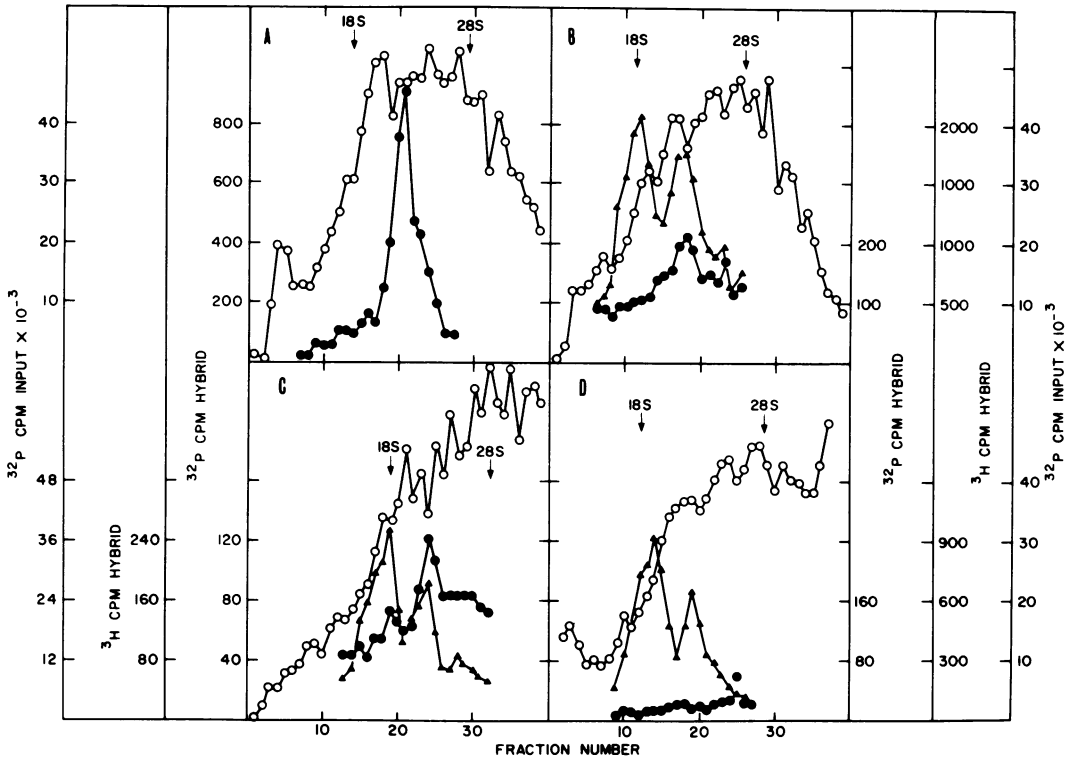


FIG. 1. Patterns of viral RNA from transformed cells. (A) Viral RNA from SV-Py3T3 cells. These cells were originally transformed with polyoma virus and then additionally transformed with SV40 virus (G. Todaro).  $25 \times 10^6$  cells were labeled for 6 h with  $100 \mu\text{Ci}$  of  $^{32}\text{PO}_4$  per ml in medium containing  $10^{-5}$  M  $\text{PO}_4$ . The phenol-extracted RNA was passed through a poly(U) filter, and the RNA which eluted from the filter was run on an acrylamide gel (2.6% acrylamide, 5 mA/gel, 9 h; ref. 41). Each gel fraction was incubated 18 h in  $2 \times \text{SSC} + 0.5\%$  SDS with a filter containing  $0.5 \mu\text{g}$  of denatured SV40 DNA. The filters were then treated with  $20 \mu\text{g}$  of pancreatic RNase per ml, and the radioactivity remaining on the filter was counted. Symbols: O, profile of RNA eluted from poly(U) filter; ●, profile of radioactivity hybridizing to SV40 filter. (B) Viral RNA from virus-free BSC/SV cells. SV40-transformed BSC-1 cells, provided by N. Goldblum (16), were labeled as in (A) with  $^{32}\text{PO}_4$ . Poly(U)-purified RNA from these cells was co-electrophoresed with  $^3\text{H}$ -labeled RNA from SV40-infected BSC-1 cells labeled 38 to 48 h postinfection with  $100 \mu\text{Ci}$  of  $[^3\text{H}]\text{uridine}$  per ml. Symbols: O, Profile of BSC/SV  $^{32}\text{P}$ -labeled RNA eluted from poly(U); ●, profile of SV40-hybridizable BSC/SV RNA; ▲,  $^3\text{H}$ -labeled late lytic viral homologous RNA. (C) Viral RNA from SV40-transformed Chinese hamster embryo cells. Transformed cells (M. Vogt) were labeled as in (A) and the RNA was co-electrophoresed with  $^3\text{H}$ -labeled RNA from cells late in lytic infection. Symbols: O, Chinese hamster embryo  $^{32}\text{P}$ -labeled RNA eluted from poly(U); ●, SV40-hybridizable RNA from Chinese hamster embryo cells,  $^{32}\text{P}$ -labeled; ▲,  $^3\text{H}$ -labeled viral homologous RNA from cells late in lytic infection. (D) Absence of hybridizable RNA from nontransformed 3T3 cells. Cells were labeled and RNA was prepared as in (A).  $[^3\text{H}]\text{RNA}$  from cells late in lytic infection was co-electrophoresed as marker. Symbols: O, Profile of  $[^{32}\text{P}]\text{RNA}$  [eluted from poly(U)] from nontransformed 3T3 cells; ●, SV40-hybridizable  $^{32}\text{P}$ -labeled RNA; ▲, late lytic virus-homologous RNA,  $^3\text{H}$ -labeled.

ref. 32). From 8 to 14 h postinfection, a time period before the onset of viral DNA replication in these cells (1), only one major species of viral RNA was apparent (Fig. 2b). A similar species was also seen in cytosine arabinoside-treated cells (Fig. 2c). This early RNA migrated on the gel halfway between 18 and 28S rRNA's and was similar in its molecular weight to the viral RNA found in transformed cells. This RNA species was also more than large enough to contain all of the viral sequences transcribed early in the

lytic cycle. The SV40-specific RNA species seen in Fig. 2b contained about  $5 \times 10^{-5}$  of the total labeled RNA in the infected cell early in the lytic cycle.

**Late lytic RNA.** Late lytic RNA consists of two prominent species of RNA. This was demonstrated in previous work, and is seen in Fig. 1 and 2, which included profiles of late lytic viral RNA as reference markers (Fig. 1B, C, D). After a 6- to 8-h label, the two late lytic species consist of one RNA species which migrates

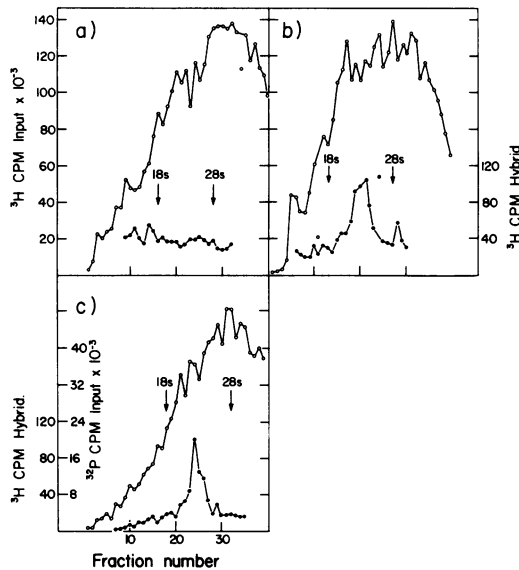


FIG. 2. Early lytic SV40 RNA. (a and b) RNA from BSC-1 cells labeled early in the lytic cycle. For each preparation,  $25 \times 10^6$  BSC-1 cells were infected at 100 PFU/cell and labeled for the indicated period with 100  $\mu$ Ci of [ $^3$ H]uridine per ml. (a) Cells labeled from 1 to 8 h postinfection. (b) Cells labeled from 8 to 14 h postinfection. Symbols:  $\circ$ ,  $^3$ H-labeled RNA eluted from poly(U) filter;  $\bullet$ ,  $^3$ H-labeled virus homologous RNA. (c) Viral RNA from cytosine arabinoside-treated cells.  $25 \times 10^6$  African green monkey kidney cells were infected with 50 PFU of virus per cell. After adsorption of virus for 1 h, cytosine arabinoside was added to a concentration of 12.5  $\mu$ g/ml. Eleven hours postinfection the cells were starved of phosphate for 2 h in phosphate-free medium plus cytosine arabinoside. They were then labeled for 7 h, and the RNA was prepared as in Fig. 1A. Symbols:  $\circ$ , [ $^{32}$ P]RNA eluted from poly(U);  $\bullet$ ,  $^{32}$ P-labeled virus homologous RNA.

approximately with 18S rRNA and a second larger species which migrates about halfway between 18 and 28S rRNA's. In previous reports (42, 43), it was demonstrated that these two late species are found largely in the cytoplasmic fraction and that at least some of these molecules contain poly(A) tails. More refined measurements, not shown here, now indicate that these species are found solely in the cytoplasm, and virtually all RNA molecules of these two types contain poly(A) tails. After extensive search, we have been unable to detect any smaller, long-lived, cytoplasmic species of viral RNA present in the late lytic cycle. Work on the related polyoma virus indicates an almost identical pattern of long-lived late viral RNA (R. A. Weinberg, Z. Ben-Ishai, and P. Rudland, unpublished observations).

After a 6- to 8-h labeling period, a profile of late viral RNA shows the smaller viral species with a peak height of 1.5 to 2 times the height of the peak of the larger RNA species. An analysis of total infected RNA (nuclear + cytoplasmic) from infected cells shows these two cytoplasmic viral RNAs above a low, heterogeneous background of viral RNA which is of nuclear origin. Shorter labeling periods, however, produce a greatly different profile of viral RNA. In Fig. 3, cells were labeled late in the lytic cycle for 3 h (Fig. 3A), and samples were exposed to actinomycin for a further 2.5 or 5 h (Fig. 3B, C). Total cellular (nuclear + cytoplasmic) RNA was extracted at each time point, fractionated by gel electrophoresis, and analyzed as before by hybridization to SV40 DNA. The larger late RNA was metabolically more labile than the smaller (Fig. 3). Although the large RNA initially predominated, after the 5-h "chase" in actinomycin, the profile of viral RNA was similar to that seen after a 6-h continuous exposure to [ $^3$ H]uridine. In addition, both peaks shifted in position during the actinomycin chase. The peak of smaller RNA moved from the right of the 18S rRNA marker to its left. The peak of larger RNA moved two fractions to the left during the actinomycin chase.

Figure 3 described the labeling kinetics of whole cell (nuclear + cytoplasmic) RNA. The changes in the proportion and size of the RNA species seen in Fig. 3 apparently took place after these RNAs entered into the cytoplasm (Fig. 4). Infected cells were exposed to  $^{32}$ PO $_4$  for 10 h, placed in non-radioactive medium for 1 h, and then labeled with [ $^3$ H]adenosine for another 2.5 h. The cells were then fractionated into cytoplasmic and nuclear fractions (Fig. 4). Both the shift in electrophoretic mobility of the smaller of the two RNA species and the change in ratio between the amounts of the two RNA species can be observed in the cytoplasmic RNA. The nuclear fraction did not contain significant amounts of either the long- or short-labeled RNA species. This experiment indicates that the decrease in molecular weight of the smaller (and probably larger) viral RNA takes place in the cytoplasm. Additionally, the change in the ratio of the amounts of the larger and smaller RNA species observed in Fig. 3 was the result of metabolism of RNA species which had arrived in the cytoplasm before this change had taken place.

The relationship between the lytic viral RNA species was further explored by hybridization of these RNAs to DNA from different portions of the SV40 genome. These DNA fragments were

prepared by cleavage of the viral genome with the restriction enzyme endonuclease Z derived from *Haemophilus aegyptius* (7). A partial characterization of the endonuclease Z fragments of SV40 has been reported (7). We have done a preliminary ordering of the fragments generated by this endonuclease (E. S. Huang, C. Mulder, and J. E. Newbold, unpublished observations). This characterization has now been extended by K. N. Subramanian, B. S.

Zain, S. M. Weissman, and J. Pan, who have mapped these fragments relative to the cuts made by the R1 and *H. influenzae* endonucleases (personal communication).

Infected cells were exposed for 13 h to  $^{32}\text{P}$ -containing medium, which was then replaced for 1 h with non-radioactive medium. The cells were then exposed for 1.5 h to medium containing  $^3\text{H}$ uridine. Only the cytoplasmic fraction was analyzed, since the previous experiment

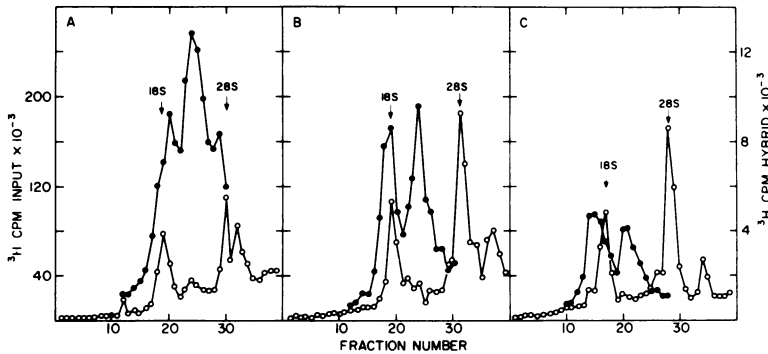


FIG. 3. Pulse-chase of viral RNA by using actinomycin D. BSC-1 cells were infected at 100 PFU/ml. At 24 h postinfection, three cultures were labeled with 100  $\mu\text{Ci}$  of  $^3\text{H}$ uridine per ml. After 3 h of labeling, total cellular RNA was extracted from one culture and actinomycin was added to the other two cultures to a concentration of 10  $\mu\text{g}/\text{ml}$ . After 2.5 h of exposure to actinomycin, total cellular RNA was extracted from the second culture and, after 5 h of exposure to actinomycin, total cellular RNA was extracted from the third culture. RNA from each culture was run directly on an acrylamide gel, and the RNA from each fraction was tested for SV40 homologous RNA. (A) Culture labeled for 3 h with  $^3\text{H}$ uridine; (B) culture labeled for 3 h with  $^3\text{H}$ uridine and then chased for 2.5 h with actinomycin; (C) culture labeled for 3 h with  $^3\text{H}$ uridine and then chased for 5 h with actinomycin. Symbols:  $\circ$ , total RNA from each culture;  $\bullet$ , SV40-hybridizable RNA.

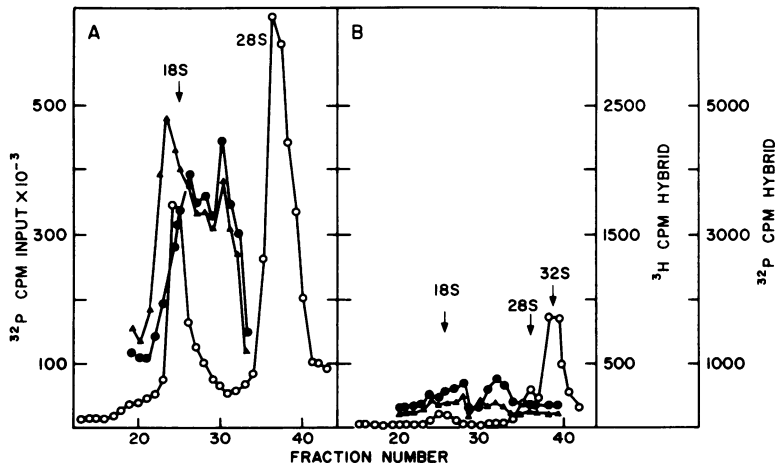


FIG. 4. Long- and short-labeled viral RNA from nucleus and cytoplasm. One culture of BSC-1 cells 60 h post-infection was labeled for 10 h with 100  $\mu\text{Ci}$  of  $^{32}\text{P}$  per ml as in Fig. 1A, placed in non-radioactive medium for 1 h, and then labeled for another 2.5 h with  $^3\text{H}$ adenosine at a concentration of 125  $\mu\text{Ci}/\text{ml}$ . The cells were fractionated according to Penman (25), and the nuclear and cytoplasmic RNAs were run directly on a gel. The gel fractions were then tested for SV40-hybridizable RNA. (A) Cytoplasmic RNA; (B) nuclear DNA. Symbols:  $\circ$ ,  $^{32}\text{P}$ -labeled whole nuclear or cytoplasmic RNA;  $\blacktriangle$ ,  $^{32}\text{P}$ -long-labeled SV40 RNA;  $\bullet$ ,  $^3\text{H}$ -short-labeled SV40 RNA.

(Fig. 4) indicated that the short- and long-labeled discrete species were located in that cell fraction. The cytoplasmic RNA was extracted with phenol-chloroform and poly(A)-containing RNA purified via poly(U) filters. The resulting

poly(A)-containing RNA was fractionated by electrophoresis through an acrylamide gel cast in 99% formamide. The pattern of poly(A)-containing RNA is shown in Fig. 5a. Three large peaks of radioactivity are seen superimposed

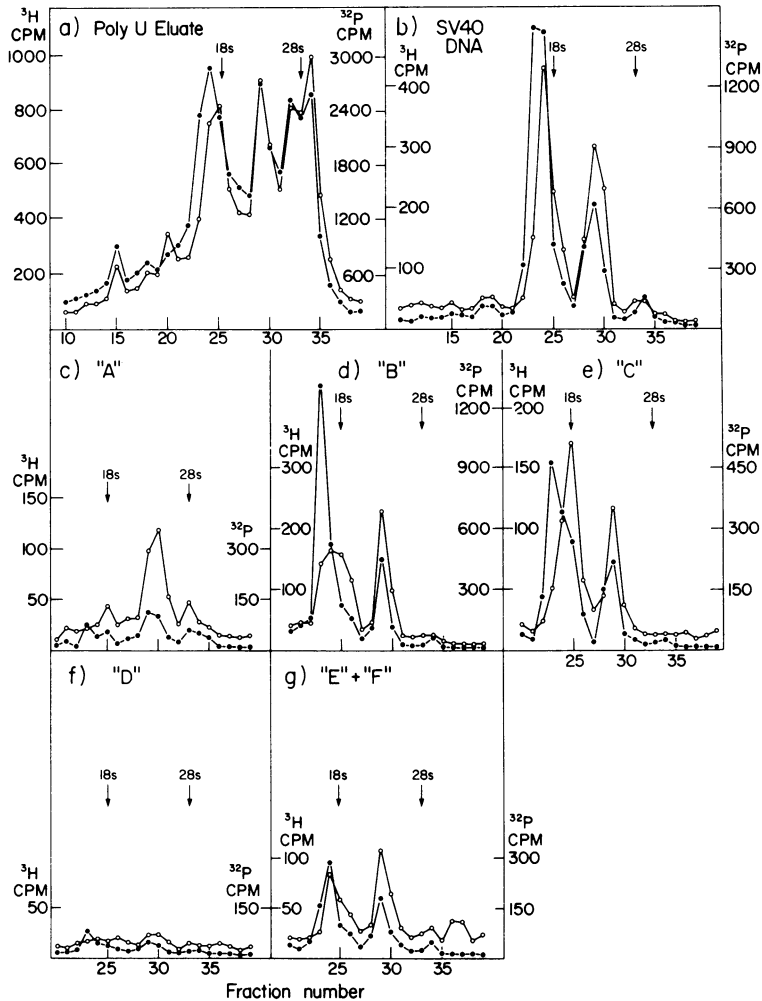


FIG. 5. Hybridization of late lytic RNA to genome fragments. Five cultures of BSC-1 cells were infected and labeled from 60 to 73 h postinfection with  $^{32}\text{PO}_4$  at a concentration of 100  $\mu\text{Ci/ml}$ . The radioactive medium was removed, and the cells were cultured for 1 h in non-radioactive medium. The infected cultures were then exposed to  $[^3\text{H}]$ -uridine at a concentration of 250  $\mu\text{Ci/ml}$  for 75 min. The cells were fractionated according to Penman's procedure (25). The cytoplasmic RNA was passed through poly(U) filters, and the poly(A)-containing RNA was eluted from these filters as before (41). The RNA was run on a 20-cm formamide gel (4) at 100 V for 15 h. The gel fractions were eluted in  $2\times \text{SSC} + 0.2\% \text{SDS}$  and boiled for 15 min to dissolve the gel and reduce the molecular weight of the RNA. (a) A 2% sample of each gel fraction was counted directly in Triton-toluene scintillant. 15% samples of each gel fraction were tested by hybridization to: (b) SV40 DNA; (c) fragment A; (d) fragment B; (e) fragment C; (f) fragment D; and (g) pooled fragments E, F<sub>1</sub> and F<sub>2</sub>. One microgram of SV40 DNA was immobilized on each of the filters used in (b). The filters of endonuclease Z fragments contained the molar equivalent of 0.7  $\mu\text{g}$  of SV40 DNA per filter, e.g., that quantity of fragment B DNA derived from cleaving 0.7  $\mu\text{g}$  of SV40 form I DNA. This amount of immobilized DNA allowed a minimum of a 60-fold excess of DNA over homologous viral RNA during the hybridization. Symbols: ●,  $^{32}\text{P}$ -long-labeled SV40 RNA; ○,  $^3\text{H}$ -short-labeled SV40 RNA.

upon a heterogeneous background. Samples of each gel fraction were tested for their ability to hybridize to SV40 DNA which was immobilized on cellulose nitrate filters. Each hybridization was performed with at least a 60-fold excess of viral DNA. The profile of SV40 homologous RNA is seen in Fig. 5b. Two of the prominent peaks seen in Fig. 5a are seen to hybridize to SV40 DNA. The third, at about 28S, was of nonviral origin. The small peaks seen in Fig. 5a (fractions 15 and 20) were also not virus specific.

The profiles of the short- and long-labeled viral RNA species at about 18S did not coincide. The shift in size of this late lytic RNA is apparent both in Fig. 5a and b, and was discussed previously (Fig. 3 and 4). The shift in size of the larger RNA species was only barely detectable here. We noted additionally a small amount of SV40 homologous RNA which migrated with a rate similar to that of the 28S rRNA marker. This RNA was of a size comparable to a complete transcript of the SV40 genome and has been observed several times upon formamide gel electrophoresis. Its small quantity precluded further study.

Although these RNAs were run in an acrylamide gel with a strongly denaturing solvent (99% formamide), their electrophoretic mobilities relative to ribosomal RNAs were quite similar to those seen in a standard acrylamide gel cast in an aqueous solvent. Earlier estimates of the molecular weight of the viral RNAs, with rRNA as molecular weight standard, were therefore unaffected in any large way by the effects which conformation might exert on the electrophoretic mobility of these molecules.

Figure 5b also demonstrates the relative metabolic stabilities of the two classes of late viral RNA. As observed previously, the larger species was metabolically less stable than the smaller.

Additional samples of the gel fractions were then hybridized to DNA fragments produced by cleavage of SV40 DNA with endonuclease Z. Having noted the different ordinate scales for each panel of Fig. 5, one can summarize the data as follows.

(i) The smaller of the late lytic RNAs (of about 18S) hybridized strongly to B and C and did not hybridize to D. Its hybridization to fragment A (Fig. 5c, fraction 25) was extremely low (10 counts/min) and probably insignificant.

(ii) The shift in position of the peaks of radioactivity between long- and short-labeled species (about 18S) is observed upon hybridization to fragments B, C, and E + F.

(iii) The  $^3\text{H}/^{32}\text{P}$  ratio measured across fractions 22 to 25 was very similar in Fig. 5d, e, and g.

(iv) The bulk of the large species hybridized to whole SV40 DNA with its peak in fraction 29 with a  $^3\text{H}/^{32}\text{P}$  ratio of 0.5 (Fig. 5b). The identical location and isotope ratio was observed upon hybridization to fragments B and C (Fig. 5d, e).

(v) Hybridization to fragment A demonstrated an RNA species which was distributed in fractions 29 and 30. In addition to migrating more slowly than the similarly sized species seen hybridizing to fragments B and C, the  $^3\text{H}/^{32}\text{P}$  ratio of this peak of radioactivity was 1.0. Therefore, this RNA species was about 50,000 daltons larger and was more rapidly labeled than the RNA species whose profile peaked in fraction 29 in Fig. 5d and e.

(vi) Of the labeled viral RNA in fractions 28 to 30 of Fig. 5b, about four times as much was homologous to fragments B + C as was homologous to fragment A.

(vii) All of these RNA species hybridized very weakly to fragment D.

Additional mapping information was provided by hybridizing late lytic RNA to ND1 DNA. ND1 is an adeno-SV40 hybrid virus containing about 17% of the SV40 genome (9, 22). The SV40 sequences contained in ND1 DNA are found in a region of the SV40 genome which straddles an early-late border (9, 13, 22, 30). Thus, hybridization of an SV40 RNA to ND1 DNA indicates that this RNA contains nucleotide sequences which can be located near this early-late border. RNA from cells labeled continuously for 6 h was run in samples on two separate acrylamide gels. These gels had been cast in standard aqueous buffer. One set of gel fractions was hybridized to SV40 DNA on filters, and the second was hybridized to ND1 DNA on filters (Fig. 6). The smaller RNA peak at about 18S hybridized well to the ND1 DNA. The larger RNA peak hybridized relatively more efficiently to SV40 than to ND1 DNA.

The evidence presented above allows a tentative mapping of SV40 transcripts (Fig. 7). This map includes the ordering of the fragments derived by Subramanian, Zain, Weissman, and Pan, who provided us with this information in advance of publication. The orientation of these fragments relative to the cut made by the R1 restriction enzyme was provided by these workers and was established independently (E. S. Huang, C. Mulder, and J. E. Newbold, unpublished observations). Also included are the results of two recent independent determinations of the location of the early and late regions of the SV40 genome (13, 30). These two recent reports have also demonstrated the direction of transcription in these regions, which is indi-

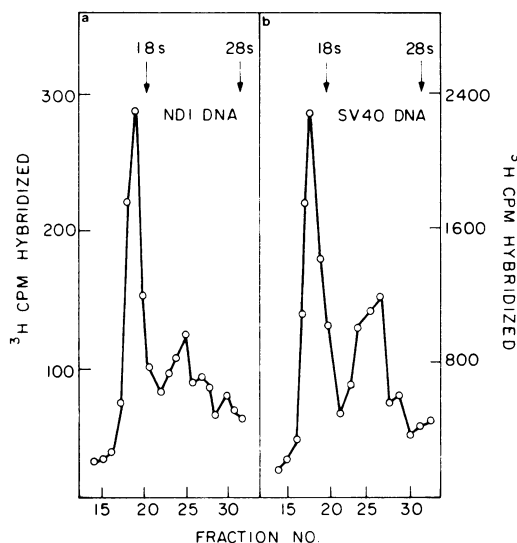


FIG. 6. Late lytic RNA hybridization to SV40 and ND1 DNAs. RNA was extracted from BSC-1 cells which were infected at 100 PFU/cell and labeled for 6 h with 100  $\mu$ Ci of [ $^3$ H]uridine per ml, beginning 48 h post-infection. Two equal samples of extracted RNA were run on separate gels on two different days, and the gel fractions were incubated under hybridizing conditions with DNA from either SV40 or ND1 virus. The fractions from one gel were incubated with filters containing 0.5  $\mu$ g of SV40 DNA, whereas the fractions from the second gel were incubated with filters containing 1.0  $\mu$ g of ND1 DNA. Symbols: ●, hybridizable counts to either SV40 or ND1 DNA. (a) Hybridization to ND1 filters; (b) hybridization to SV40 filters.

cated by the arrowheads. An additional report provides the location of the SV40 segment found in ND1 DNA (21). Although these latter three reports determined the location and direction of SV40 transcription relative to genome fragments derived by using other endonucleases, these findings and the present ones can all be normalized to one map by orientation to the R1 cleavage site. We stress that the exact location of the early-late border relative to endonuclease Z map has only been determined as being near the right end of fragment C.

## DISCUSSION

**Transformed cell viral RNA.** Evidence presented in Fig. 1 for several SV40-transformed cell lines and previous work on viral RNA in SV3T3 cells establish that the most prominent viral RNA species found in transformed cells migrates halfway between 18 and 28S rRNA's. This migration rate suggests a mass of 900,000 to 1,000,000 daltons. Of this mass, 50,000 dal-

tons must consist of a poly(A) tail which is not transcribed from the SV40 genome (42). The remaining  $0.90 \times 10^6$  to  $0.95 \times 10^6$  daltons of RNA contain more nucleotide sequences than a transcript of the early region of the SV40 genome ( $0.5 \times 10^6$  to  $0.7 \times 10^6$  daltons; 11, 13, 30, 37). Therefore, this RNA species either contains anti-late sequences or sequences which are of nonviral origin. Viral RNA covalently linked to cellular RNA (39) and viral RNA of anti-late sequence have both been reported in SV40-transformed cells (11, 24). Data presented here do not distinguish between these possibilities.

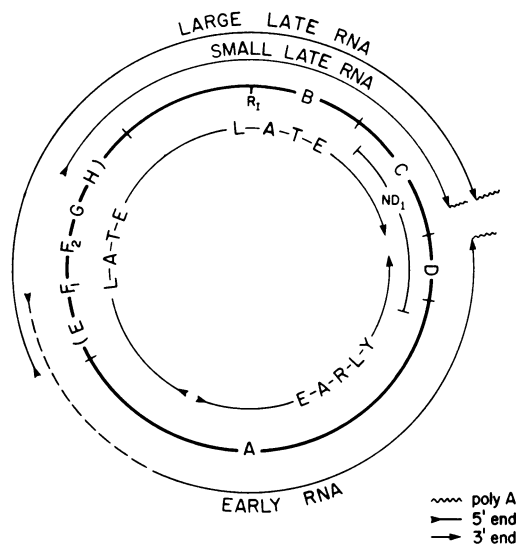


FIG. 7. Transcription map of SV40. This map is a concordance of several maps, all oriented to the R1 cleavage site. Going outwards from the innermost circle: (i) the location of the early and late regions, and the direction of transcription as determined by Khoury et al. (13) and Sambrook et al. (30); (ii) the location of the ND1 site from Morrow and Berg (21) and Morrow et al. (22); (iii) endonuclease Z fragment map, as determined by K. N. Subramanian, B. S. Zain, S. M. Weissman, and J. Pan (personal communication). The ordering of fragments E through G is still being determined. This map is confirmed in part by hybridization of adeno-SV40 viral RNAs (7) and by partial digestion studies (E. S. Huang and J. E. Newbold, unpublished observations). An additional small fragment, termed "E<sub>2</sub>" in large-plaque strain DNA and "X" in small-plaque strain DNA (7), is also located among the small fragments on the left portion of the map. (iv) The proposed location of the genome sequences complementary to the early and late transcripts. The 5' end of the early RNA is indicated as a broken line, since a portion of this RNA may not be transcribed from the viral genome. This hypothetical nonviral portion is arbitrarily placed at the 5' end of the early transcript.



The present evidence does not preclude the existence of other viral RNA species which must be present in transformed cell lines in which as much as 80% of the viral genome is transcribed (11, 24). Much of the viral RNA in such transformed cell lines must contain anti-late sequences. These anti-late sequences cannot contain information coding for proteins necessary for the maintenance of the transformed state. We would suggest that the viral RNA species of 900,000 to 1,000,000 daltons seen here is common to many SV40-transformed cell lines and related to the maintenance of the transformed state in such cells. In addition, other viral sequences may be present in these cells which are not required to keep these cells in a transformed state.

**Early RNA species.** The early RNA is of similar size to that found in several transformed cell lines. Early viral RNA and viral RNA from transformed cells compete strongly with one another and are transcribed from a similar region of the SV40 genome (1, 11). Our evidence here does not demonstrate absolute identity of molecular weight or nucleotide sequence. Several independent determinations have shown that 30 to 40% of the viral genome is transcribed early in the lytic cycle and that these same early sequences continue to be transcribed in the late lytic cycle (1, 10, 13, 23, 30, 31). Such determinations would predict an early transcript whose maximal size would be 600,000–700,000 daltons, excluding the contribution of the poly(A) tail. This molecular weight is less than the  $0.9 \times 10^6$  to  $1.0 \times 10^6$  molecular weight which we estimated for the early RNA species. Our estimates have now been derived from RNA fractionation in formamide gels in which the conformation of RNA species should have relatively little effect on their electrophoretic mobility.

Late in the lytic cycle, the bulk of the viral RNA running halfway between 18 and 28S rRNA's hybridized to late viral DNA fragments. Only a minority of this RNA hybridized to the early fragment A. This minority species differed from the bulk of viral RNA in this region of the gel (Fig. 5) in two respects. (i) The  $^3\text{H}/^{32}\text{P}$  ratio of the minority species was more than twice that of the bulk species. This indicates unequivocally that it is more rapidly labeled than the bulk RNA species. (ii) Its electrophoretic mobility was less than that of the bulk species. This minority species is probably identical to the viral RNA which we observed early in the lytic cycle. We would argue that this viral RNA species is initially synthesized in the early portion of the virus lytic cycle. It continues to be

transcribed in the late phase of the lytic cycle (see also 1, 19, 23, 30, 31), but its presence is soon obscured by a much larger amount of late lytic transcript of similar molecular weight. The present evidence suggests that this early viral RNA species represents 5 to 10% of the total viral RNA present in the cytoplasm late in the lytic cycle. Following the mapping of Khoury et al. (13) and Sambrook et al. (30), we placed this RNA species on the genome map with its 3' end at the early/late junction near the right end of fragment C. Since the early RNA produces only a 140-counts/min peak upon hybridization to fragment A, which is 2,050 nucleotides long, its weak hybridization to fragment D (295 nucleotides long) is understandable. This early viral RNA species probably functions as the viral mRNA which specifies early viral functions such as the T, U, and TSTA antigens (22).

**Late lytic RNA.** The bulk of the viral RNA late in the lytic cycle is apparently uniquely late RNA, i.e., viral RNA sequences whose transcription begins with the initiation of viral DNA replication. As discussed above, only a minority of the viral RNA present late in the lytic cycle derives from continued transcription of early RNA. The uniquely late RNA consists of two RNA species. The small late RNA is about the same size as 18S rRNA, whereas the large late RNA migrates in acrylamide gels halfway between 18 and 28S rRNA's. We do not rule out the existence of very small amounts of other late viral RNA transcripts in the cytoplasm.

These two late RNAs have sequences in common. This is shown by several lines of evidence. (i) Both RNAs hybridize to fragments B, C, and E + F. (ii) They compete with each other for the same viral DNA sequences (E. Winocour, personal communication). (iii) Both RNAs can hybridize to, and thus are complementary to, the viral RNA synthesized *in vitro* by transcription of viral DNA with *Escherichia coli* RNA polymerase (D. M. Lindstrom and R. Weinberg, unpublished observations). This *in vitro* synthesized RNA has been shown to be complementary to the bulk of late *in vivo* transcripts (15). (iv) The two late species hybridize to a region of the viral genome which has been shown to specify *in vivo* cytoplasmic transcripts which are complementary only to the L strand of the viral genome (13, 30).

Present evidence does not absolutely preclude the existence of several different small late RNA species, each of about 18S, each of which hybridizes to B and C, and each of which begins and ends at a different site on the viral genome. The hybridization to fragments B, C, E + F,

and ND1 DNA is, however, most compatible with one small late RNA species with a unique 5' end.

The large late RNA species is probably large enough to encompass almost the entire late region. It appears to be about 50,000 daltons smaller than the early RNA. For purposes of simplicity, we tentatively place the 3' end of the large late RNA coterminous with the 3' end of the small late RNA.

Others have recently reported differences in fingerprints of T1 digests of the small and large late RNAs (40). We would suggest that these differences derive from that portion of the large late RNA which is not shared in common with the small late RNA.

Both late viral RNA species are located almost solely in the cytoplasm, where they probably function as mRNA's. The larger RNA is metabolically less stable than the smaller late RNA. By using short-labeling protocols (Fig. 3a and b), the larger species can be seen to predominate, whereas after long periods of labeling the smaller viral RNA had a peak height 1.5 to 2 times that of the larger. After short labeling periods which are followed by very long chases, the smaller late RNA can be seen to predominate by a factor of three or four (not shown). This kinetic evidence and the common sequences shared by these two RNAs are all consistent with a precursor-product relationship between the large and small late RNAs. Such a relationship has not yet been proven, however.

The exact mapping of the 5' ends of the late viral RNAs is presently complicated by the absence of a map of the small fragments. These small fragments (E, F<sub>1</sub>, F<sub>2</sub>, G, and H) are clustered in one region of the viral genome. We hybridized viral RNA to pooled fragments E, F<sub>1</sub>, and F<sub>2</sub> (Fig. 5g), which together contain 13.5% of the viral genome. Until these and the other small fragments have been ordered, the meaning of the relative peak heights in Fig. 5g remains obscure.

The smaller late RNA decreased noticeably in size with increased labeling time. A more subtle decrease in size can also be detected for the large late lytic species. This phenomenon may be attributable to a time-dependent decrease in length of the poly(A) tail of these RNA species. A similar decrease in size of cell mRNA with increased labeling time has been linked to the observed shortening of the poly(A) of cellular mRNA (5, 20, 34, 36).

**An unresolved problem.** A striking paradox in the present data derives from the large molecular weight of the early transcript. This

cytoplasmic RNA has a mass of 900,000 to 1,000,000 daltons, which is far larger than the transcript from the 30 to 35% of the genome allotted to early functions. It is therefore conceivable that the early viral RNA contains a section of nonviral sequences covalently linked to those viral sequences specified by the early part of the viral genome. Hybrid RNA molecules of mixed viral-cell sequence have in fact been reported in the SV40 lytic infection (28), but such hybrid molecules are largely confined to the nucleus. If early mRNA and the transformed mRNA's do contain a section of nonviral sequence, then the RNA from each source would be unique, differing from the others in these sequences of nonviral origin.

#### ACKNOWLEDGMENTS

R. A. W. was a fellow of the Helen Hay Whitney Foundation. Z. B.-I. was supported by Public Health Service international postdoctoral research fellowship 5F05 TWO p646-02 from the Fogarty International Center. This work was supported in part by grants from the Public Health Service (5R01 CA07592-09 from the National Cancer Institute and general research support award 5 SO-RR-05406), the University Research Council of the University of North Carolina, and by Public Health Service grant 5 RO 1CA14572.

We would like to thank A. M. Lewis, Jr. for giving us a stock of ND1 adeno-SV40 hybrid and sample of its purified DNA. M. Vogt and N. Goldblum are thanked for giving us SV40-transformed lines. K. N. Subramanian, B. S. Zain, S. M. Weissman, and J. Pan kindly provided us with a map of the endonuclease Z fragments of the SV40 genome in advance of publication. We would also like to thank R. Dulbecco for generously providing facilities and advice during the first half of the work which was carried out at the Salk Institute, La Jolla, Calif.

#### ADDENDUM IN PROOF

P. Lebowitz, W. Siegel, and J. Sklar (personal communication) have recently derived a more detailed map of the *Haemophilus influenzae* endonuclease fragments of SV40 DNA which confirms the mapping reported here.

#### LITERATURE CITED

- Aloni, J., E. Winocour, and L. Sachs. 1968. Characterization of the simian virus 40-specific RNA in virus yielding and transformed cells. *J. Mol. Biol.* 31:415-429.
- Butel, J. S., and F. Rapp. 1965. The effect of arabinofuranosyl-cytosine on the growth cycle of simian virus 40. *Virology* 27:490-495.
- Danna, K. J., G. H. Sack, Jr., and D. Nathans. 1973. Studies of simian virus 40 DNA. VII. A cleavage map of the SV40 genome. *J. Mol. Biol.* 78:363-376.
- Duesberg, P. H., and P. K. Vogt. 1973. Gel electrophoresis of avian leukosis and sarcoma virus RNA in formamide: comparison with other viral and cellular RNA species. *J. Virol.* 12:594-599.
- Greenberg, J. R., and R. P. Perry. 1972. The isolation and characterization of steady-state labeled messenger RNA from L cells. *Biochim. Biophys. Acta* 287:361-366.
- Hirt, B. 1967. Selective extraction of polyoma DNA from

- infected mouse cell cultures. *J. Mol. Biol.* **26**:365-369.
7. Huang, E. S., J. E. Newbold, and J. S. Pagano. 1973. Analysis of simian virus 40 DNA with the restriction enzyme of *Haemophilus aegyptius*. *endonuclease Z. J. Virol.* **11**:508-514.
  8. Keely, T., and J. Rose. 1971. Simian virus 40 integration site in an adenovirus 7-simian virus 40 hybrid DNA molecule. *Proc. Nat. Acad. Sci. U.S.A.* **68**:1037-1041.
  9. Kelly, T. K., Jr., and A. M. Lewis, Jr. 1973. Use of nondefective adenovirus-simian virus 40 hybrids for mapping the simian virus 40 genome. *J. Virol.* **12**:643-652.
  10. Khoury, G., J. C. Byrne, and M. A. Martin. 1972. Patterns of simian virus 40 DNA transcription after acute infection of permissive and nonpermissive cells. *Proc. Nat. Acad. Sci. U.S.A.* **69**:1925-1928.
  11. Khoury, G., J. C. Byrne, K. K. Takemoto, and M. A. Martin. 1973. Patterns of simian virus 40 deoxyribonucleic acid transcription. II. In transformed cells. *J. Virol.* **11**:54-60.
  12. Khoury, G., and M. A. Martin. 1972. Comparison of SV40 DNA transcription *in vivo* and *in vitro*. *Nature N. Biol.* **238**:4-6.
  13. Khoury, G., M. A. Martin, T. N. H. Lee, K. J. Danna, and D. Nathans. 1973. A map of simian virus 40 transcription sites expressed in productively infected cell. *J. Mol. Biol.* **78**:377-389.
  14. Kit, S., D. R. Dubbs, P. M. Frearson, and J. L. Melnick. 1966. Enzyme induction in SV40 infected green monkey kidney cultures. *Virology* **29**:69-83.
  15. Lindstrom, D. M., and R. Dulbecco. 1972. Strand orientation of simian virus 40 transcription in productively infected cells. *Proc. Nat. Acad. Sci. U.S.A.* **69**:1517-1520.
  16. Margalith, M., R. Volk-Fuchs, and N. Goldblum. 1969. Transformation of BSC-1 cells following chronic infection with SV40. *J. Gen. Virol.* **5**:321-327.
  17. Martin, M. A. 1970. Characteristics of SV40 DNA transcription during lytic infection, abortive infection, and in transformed mouse cells. *Cold Spring Harbor Symp. Quant. Biol.* **35**:833-841.
  18. Martin, M. A., and D. Axelrod. 1969. SV40 gene activity during lytic infection and in a series of SV40 transformed mouse cells. *Proc. Nat. Acad. Sci. U.S.A.* **64**:1203-1210.
  19. Martin, M. A., and G. Khoury. 1973. Transcription of SV40 DNA in lytically infected and transformed cells, p. 33-50. *In* W. S. Robinson (ed.). Academic Press, Inc., New York.
  20. Mendecki, J., S. Y. Lee, and G. Brawerman. 1972. Characteristics of the polyadenylic acid segments associated with messenger RNA in mouse sarcoma 180 ascites cells. *Biochemistry* **11**:792-798.
  21. Morrow, J. F., and P. Berg. 1972. Cleavage of simian virus 40 DNA at a unique site by a bacterial restriction enzyme. *Proc. Nat. Acad. Sci. U.S.A.* **69**:3365-3369.
  22. Morrow, J. F., P. Berg, T. J. Kelley, Jr., and A. M. Lewis, Jr. 1973. Mapping of simian virus early functions at the viral chromosome. *J. Virol.* **12**:653-658.
  23. Oda, K., and R. Dulbecco. 1968. Regulation of transcription of the SV40 DNA in productively infected and in transformed cells. *Proc. Nat. Acad. Sci. U.S.A.* **60**:525-532.
  24. Ozanne, B., P. A. Sharp, and J. Sambrook. 1973. Transcription of simian virus 40. II. Hybridization of RNA extracted from different lines of transformed cells to the separated strands of simian virus 40 DNA. *J. Virol.* **12**:90-98.
  25. Penman, S. 1966. RNA metabolism in the HeLa cell nucleus. *J. Mol. Biol.* **17**:117-130.
  26. Rapp, F., J. L. Melnick, J. S. Butel, and T. Kitahara. 1964. The incorporation of SV40 genetic material into adenovirus 7 as measured by intranuclear synthesis of SV40 tumor antigen. *Proc. Nat. Acad. Sci. U.S.A.* **52**:1348-1352.
  27. Rowe, W. P., and S. G. Baum. 1964. Evidence for a possible genetic hybrid between adenovirus type 7 and SV40 viruses. *Proc. Nat. Acad. Sci. U.S.A.* **52**:1340-1347.
  28. Rozenblatt, S., and E. Winocour. 1972. Covalently linked cell and SV40-specific sequences in an RNA from productively infected cells. *Virology* **50**:558-566.
  29. Sambrook, J., P. A. Sharp, and W. Keller. 1972. Transcription of simian virus 40. I. Separation of the strands of SV40 DNA and hybridization of the separated strands to RNA extracted from lytically infected and transformed cells. *J. Mol. Biol.* **70**:57-71.
  30. Sambrook, J., B. Sugden, W. Keller, and P. A. Sharp. 1973. Transcription of simian virus 40. III. Mapping of "early" and "late" species of RNA. *Proc. Nat. Acad. Sci. U.S.A.* **70**:3711-3715.
  31. Sauer, G. 1971. Apparent differences in transcriptional control in cells productively infected and transformed by SV40. *Nature N. Biol.* **231**:135-138.
  32. Sauer, G., and J. R. Kidwai. 1968. The transcription of the SV40 genome in productively infected and transformed cells. *Proc. Nat. Acad. Sci. U.S.A.* **61**:1256-1263.
  33. Sharp, P. A., B. Sugden, B., and Sambrook, J. 1973. Detection of two restriction endonuclease activities in *Haemophilus parainfluenzae* using analytical agarose-ethidium bromide electrophoresis. *Biochemistry* **12**:3055-3063.
  34. Sheiness, D., and J. E. Darnell. 1973. The polyadenylic acid segment becomes shorter with age. *Nature N. Biol.* **241**:265-268.
  35. Sheldon, R., C. Jurale, and J. Kates. 1972. Detection of polyadenylic acid sequences in viral and eukaryotic RNA. *Proc. Nat. Acad. Sci. U.S.A.* **69**:417-421.
  36. Singer, R. H., and S. Penman. 1973. Messenger RNA in HeLa cells kinetics of formation and decay. *J. Mol. Biol.* **78**:321-334.
  37. Tai, H. T., C. A. Smith, P. A. Sharp, and J. Vinograd. 1972. Sequence heterogeneity in closed simian virus 40 deoxyribonucleic acid. *J. Virol.* **9**:317-325.
  38. Tonegawa, S., G. Walter, A. Bernardini, and R. Dulbecco. 1970. Transcription of the SV40 genome in transformed cells and during lytic infection. *Cold Spring Harbor Symp. Quant. Biol.* **35**:823-831.
  39. Wall, R., and J. E. Darnell. 1971. Presence of cell and virus specific sequences in the same molecules of nuclear RNA from virus transformed cells. *Nature N. Biol.* **232**:73-75.
  40. Warnaar, S. O., and A. W. de Mol. 1973. Characterization of two simian virus 40-specific RNA molecules from infected BSC-1 cells. *J. Virol.* **12**:124-129.
  41. Weinberg, R., M. Willems, U. Loening, and S. Penman. 1967. Acrylamide gel electrophoresis of HeLa cell nucleolar RNA. *Proc. Nat. Acad. Sci. U.S.A.* **58**:1088-1095.
  42. Weinberg, R. A., Z. Ben-Ishai, and J. E. Newbold. 1972. Poly A associated with SV40 messenger RNA. *Nature N. Biol.* **238**:111-113.
  43. Weinberg, R. A., S. O. Warnaar, and E. Winocour. 1972. Isolation and characterization of simian virus 40 ribonucleic acid. *J. Virol.* **10**:193-201.